

Supporting Information for

Mechanistic Insight into Proton-Coupled Mixed Valency

Luke A. Wilkinson,^{a,b} Kevin B. Vincent,^a Anthony J. H. M. Meijer^b and Nathan J. Patmore^{*a}

a) Department of Chemical Sciences, University of Huddersfield, Huddersfield HD1 3DH, UK

b) Department of Chemistry, University of Sheffield, Sheffield S3 7HF, UK

Table of contents

Experimental

<i>General considerations</i>	S2
<i>Materials</i>	S2
<i>Synthetic procedures</i>	S3
<i>Computational details</i>	S4
Scheme S1. Bond lengths calculated for $[\mathbf{I}']_2$, and the DPT and SPT1 products.	S5
Figure S1. IR spectra of $[\mathbf{I}]_2$, $[\mathbf{I}]_2^+$ and $[\mathbf{I}]_2^{2+}$.	S6
Figure S2. Cyclic voltammograms of $[\mathbf{I}]_2$ and $[\mathbf{I-D}]_2$.	S7
Figure S3. Spin density plot for $[\mathbf{I}']_2^+$.	S8
Figure S4. Calculated potential energy surface associated with DPT.	S9
Figure S5. Changes in dipole associated with the SPT1 and SPT2.	S10
Figure S6. Cyclic voltammogram of $[\mathbf{I}]_2$ recorded in the spectroelectrochemical cell.	S11
Table S1. Calculated atomic coordinates for $[\mathbf{I}']_2^+$.	S12
References	S13

Experimental

General Considerations

The synthesis and manipulation of D₂DOP, [I]₂ and [I-D]₂ was performed under inert atmosphere using standard Schlenk line and glove-box techniques. The NMR measurements were taken on a Bruker AVIII 400MHz spectrometer using solvents (CD₂Cl₂, CDCl₃, (CD₃)₂SO) that were vacuum distilled over CaH₂. Electrochemical studies were carried out using an Autolab PGSTAT 100N potentiostat in an N₂-purged solution of the electrolyte NBu₄PF₆ (0.1 M). In each case, a standard three-electrode setup was implemented with a platinum disk working electrode, a platinum wire as a counter electrode and a Ag/AgCl electrode as a pseudo-reference. After each experiment, a small amount of ferrocene was added as an internal reference and all data is reported versus the Fc/Fc⁺ couple. All potentials are reported for a scan rate of 100 mV/s unless otherwise stated. The EPR measurements were carried out at X-band using a JEOL JES-FA100 EPR spectrometer. The radical cations Mo₂(TiPB)₄⁺ and [I]₂⁺ were prepared by one equivalent of AgPF₆ to the sample in DCM immediately prior to measurement.

IR spectroelectrochemical measurements were taken using a Jasco FTIR-4100 IR spectrometer, fitted with a spectroelectrochemical cell with CsF windows and a variable temperature cell holder purchased from Specac. The cell was charged inside a glovebox with a mixture of [I]₂ (20 mM) dissolved in a 0.1 M ⁿBu₄NPF₆ / CH₂Cl₂ solution. The cell was cooled to -30 °C, and the applied cell potential was increased in small steps (50-100 mV), with the system allowed to equilibrate before each increment. When complete oxidation had occurred, as evidenced by the relative changes in the spectral profile, the potential was reversed to determine the chemical reversibility of the experiment. Comparison of the spectrum associated with [I]₂ before and after the experiment showed that ~75 % of [I]₂ was recovered indicating a small amount of decomposition of the radical cation.

Materials

3,6-Dihydropyridazine and DCl (20 % in D₂O) were obtained from commercial sources and used as received. Tetra-n-butylammonium hexafluorophosphate was

obtained from Tokyo chemical industries and was recrystallized from hot ethanol prior to use. All solvents (with the exception of MeOH) were purified by distillation over CaH₂, and degassed with argon or with the freeze-pump-thaw method. Methanol was distilled over magnesium methoxide and degassed in a similar fashion. Freshly prepared solutions of sodium methoxide were made by addition of sodium metal to dry methanol.

Synthetic procedures

Synthesis of D₂DOP. 3,6-dihydroxypyridazine (1.30 g, 11.4 mmol) was placed in a Schlenk tube and heated at 80°C under vacuum for 2 hours to remove any moisture. After cooling, and under an inert atmosphere, methanol was added to produce a colourless slurry. Freshly prepared NaOMe (22.8 mL, 1 M) was added dropwise and the mixture stirred overnight. Methanol was removed *in vacuo*, and the salt dried at 60 °C under vacuum overnight to remove excess solvent. The dry salt was then transferred to a separate Schlenk tube into which D₂O (10 mL) was added. After heating to 60°C and stirring, the salt dissolved and (under a flow of argon) 10 mL of DCl (20%) in D₂O was added via pipette. The reaction was stirred for 30 mins and then cooled to room temperature, and the product isolated via filtration to obtain D₂DOP in good yield (1.2 g, 11 mmol, 88 %). ¹H NMR spectroscopy indicated 98% conversion to D₂DOP.

Synthesis of [Mo₂(TiPB)₃(DDOP)]₂, ([I-D]₂). The synthesis of [I-D]₂ followed the same procedure as for [I]₂.¹ Mo₂(TiPB)₄ (0.236 g, 0.20 mmol) and D₂DOP (0.023 g, 0.20 mmol) were stirred together in toluene for two days. The solvent was removed *in vacuo* and hexane added. Centrifugation yielded a purple precipitate which was isolated by decanting off the mother liquor, then dried *in vacuo* (0.130 g, 0.12 mmol, 62%).

The ¹H NMR spectrum of [I-D]₂ in CD₂Cl₂ was identical to that of [I]₂, with the exception of the intensity associated with the N-H proton at δ = 11.82. This peak should have been absent in [I-D]₂, but some residual protio impurity was present, with integrals indicating that the product was a 7:3 mixture of I-D and I. No evidence of

proton containing impurities were observed in the ^1H NMR of the starting materials, so the reaction was repeated in CH_2Cl_2 and CD_2Cl_2 , in case the protio impurity was coming from the toluene solvent, however a similar mixture of products was obtained. The presence of **I** even when the reaction is performed in deuterated solvent suggests that the protio impurity may come from exchange with the TiPB^- ligands. However, the degree of deuteration is sufficient enough to observe possible changes in the cyclic voltammogram of $[\text{I-D}]_2$.

Computational details

Molecular structure calculations were performed using density functional theory as implemented in the Gaussian 09 software package.² The M06 functional³ and the 6-311G(d,p) basis set⁴ were used for H, C, O, and N, along with the SDD energy consistent pseudopotentials⁵ for molybdenum. All geometry optimizations were performed as unrestricted open shell calculations without symmetry constraints in a CH_2Cl_2 solvent cavity using the polarizable continuum model, as implemented in Gaussian 09. The HDOP ligands in $[\text{Mo}_2(\text{O}_2\text{CH})_3(\text{HDOP})]_2^+$ ($[\text{I}']_2^+$) were found to adopt the lactam-lactam tautomeric form in the ground state. The geometry was confirmed to be a minimum on the potential energy surface by frequency analysis, and calculated atomic coordinates are given in Table S1.

The geometry of the lactim-lactim product resulting from double proton transfer (DPT) and one of the lactam-lactim products resulting from single proton transfer (SPT1) were fully optimized. The geometry of the second lactam-lactim tautomer (the SPT2 product) could not be refined as the electron hole was transferred to the other dimolybdenum unit regardless of starting geometry. Key calculated structural parameters for $[\text{I}']_2^+$ and the SPT1 and DPT products are summarized in Scheme S1. In order to calculate the potential energy surface associated with single or double proton transfer, the coordinates of the $[\text{I}']_2^+$ ground state was used as the starting geometry. For SPT1 and SPT2, full geometry optimizations were performed at regular intervals along the proton transfer coordinate by constraining the N-H bond length to increase at 0.05 Å intervals. Further points were included along the SPT2 potential energy surface to locate the point at which electron transfer occurs. For DPT, concerted proton transfer was modeled by constraining both N-H bond distances as they moved along the potential energy surface.

Scheme S1. Selected bond lengths (Å) calculated for $[\mathbf{I}']_2^+$, and the DPT and SPT1 products.

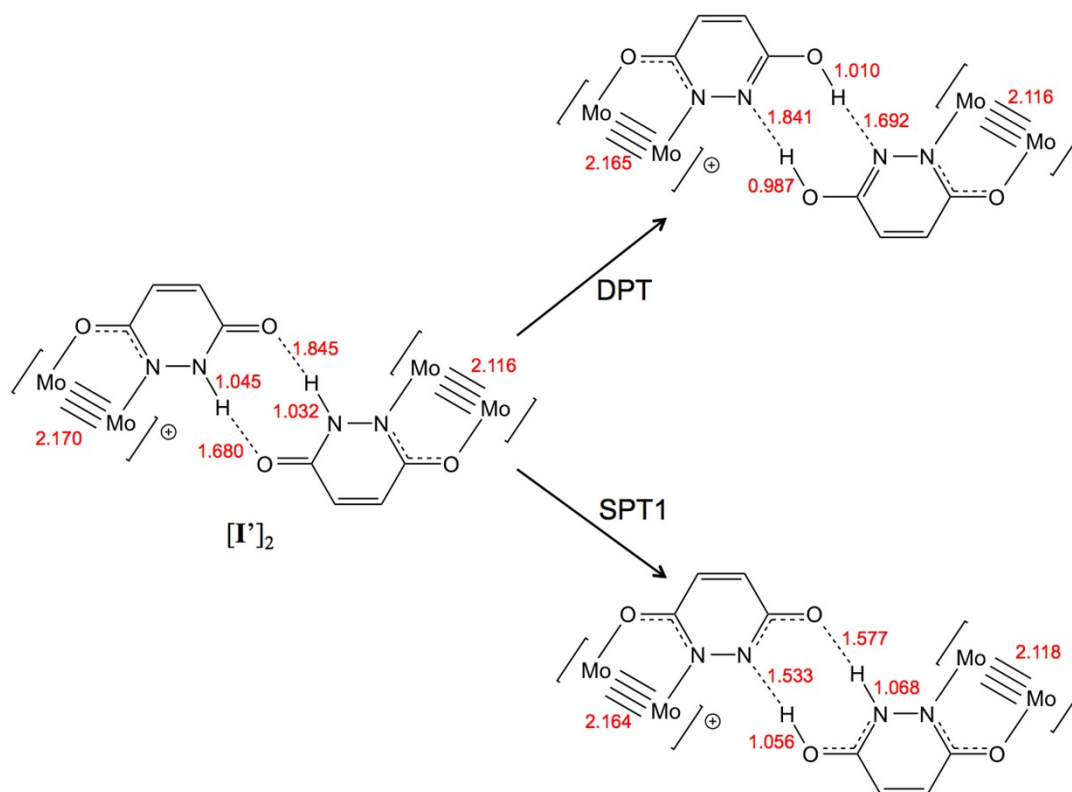


Figure S1. IR spectra of 20 mM solutions $[I]_2$ (red), $[I]_2^+$ (green) and $[I]_2^{2+}$ (blue) recorded in 0.1 M NBu_4PF_6 / CH_2Cl_2 at $-30\text{ }^\circ\text{C}$ using a spectroelectrochemical cell. Gaps in spectra are due to intense solvent absorptions.

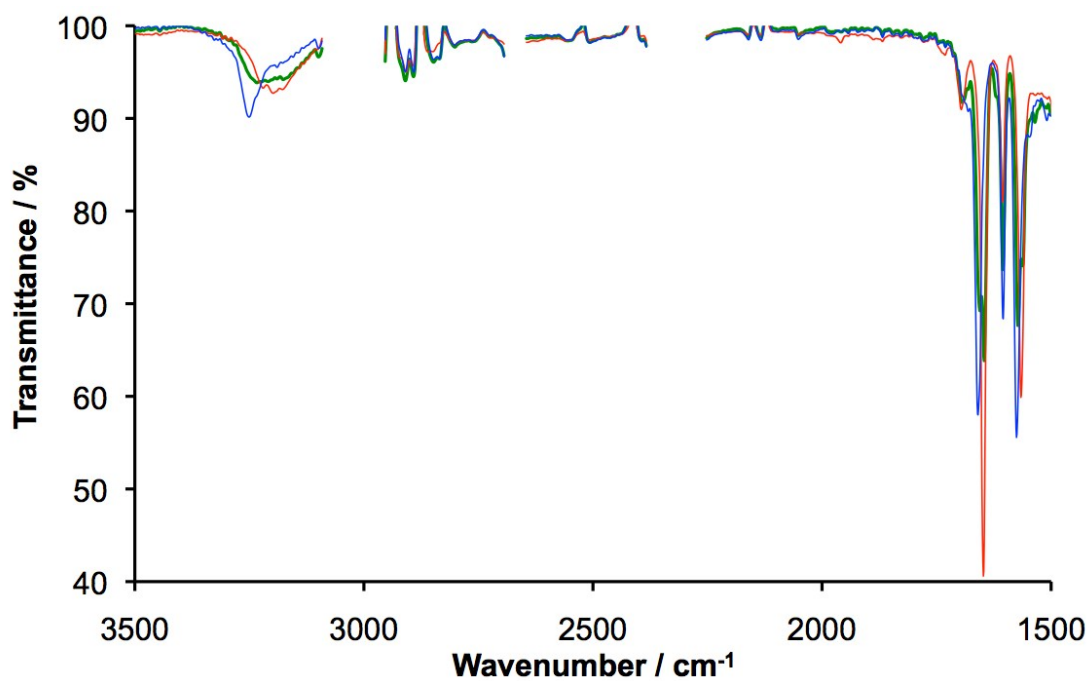


Figure S2. Cyclic voltammogram of $[I]_2$ (bottom) and $[I-D]_2$ (top) at 5 mM concentration recorded in 0.1 M NBu_4PF_6 / CH_2Cl_2 solutions at room temperature (scan rate = 100 mV s^{-1}).

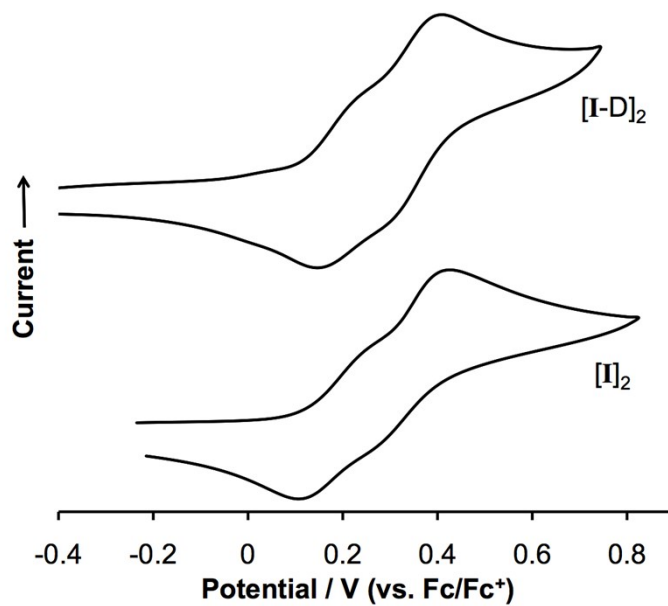


Figure S3. Spin density plot for $[\mathbf{I}']_2^+$.

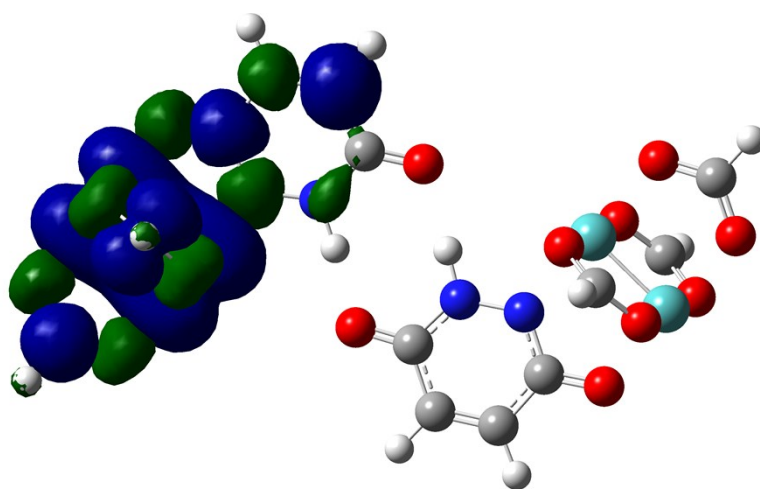


Figure S4. Calculated potential energy surface associated with concerted double proton transfer in $[\mathbf{I}']_2$.

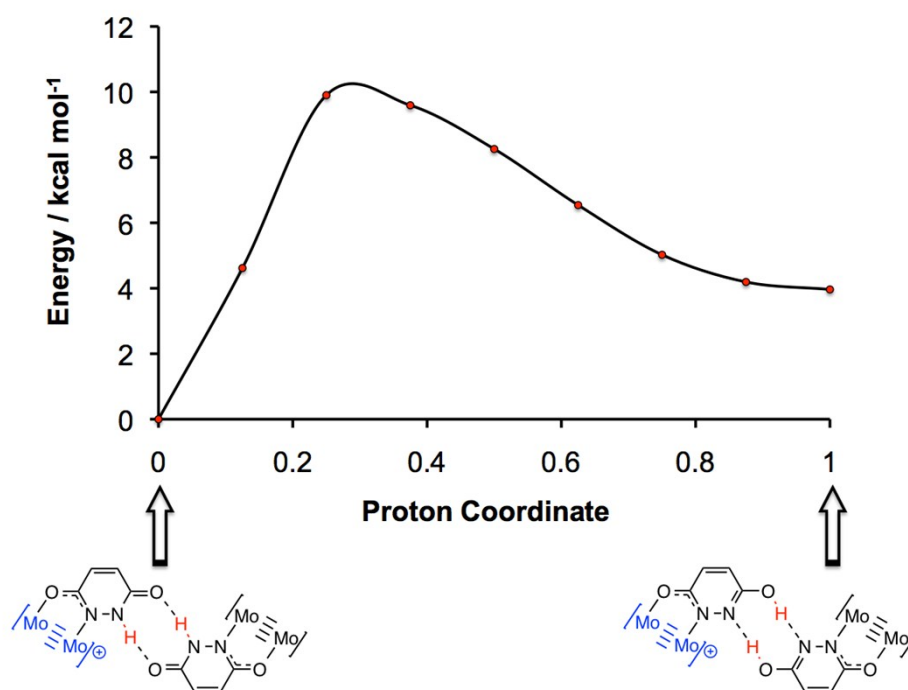


Figure S5. Changes in dipole associated with the SPT1 (red) and SPT2 (blue) potential energy surfaces.

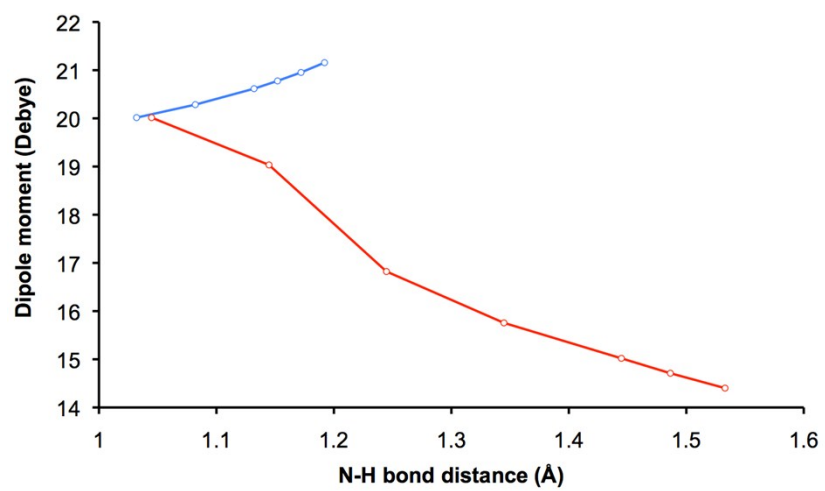


Figure S6. Cyclic voltammogram of [I]₂ recorded in the spectroelectrochemical cell in a 0.1 M NBu₄PF₆ / CH₂Cl₂ solution at -30 °C (scan rate = 50 mVs⁻¹).

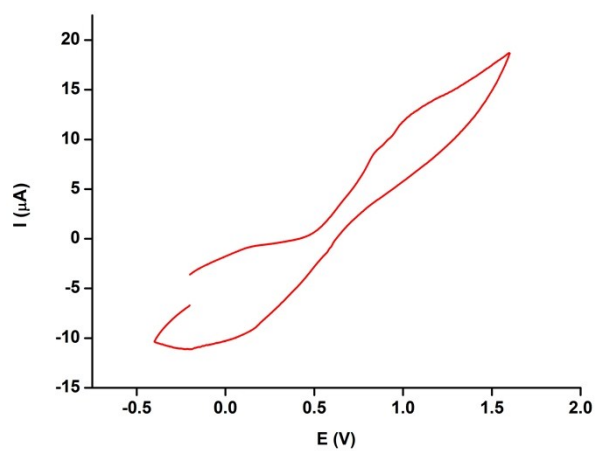


Table S1. Calculated atomic coordinates for $[\text{I}']_2^+$.

Center Number	Atomic Number	Coordinates (Angstroms)		
		x	y	z
1	1	-0.711663	4.216827	-0.492075
2	1	-3.209278	4.382989	-0.330651
3	6	-1.348452	3.342325	-0.425187
4	6	-2.686053	3.433874	-0.339216
5	6	-0.688421	2.044297	-0.437173
6	6	-3.474443	2.24126	-0.239091
7	6	-4.6791	0.11011	2.781533
8	8	-4.757232	2.287251	-0.123318
9	8	-5.642577	0.714745	2.237539
10	6	6.692574	2.14313	0.491327
11	7	-2.885885	1.045234	-0.248306
12	8	5.467509	2.389415	0.345625
13	6	4.652331	-0.179822	2.773316
14	8	-3.835947	-0.567498	2.134734
15	8	3.866417	0.566303	2.132135
16	8	7.18049	0.983004	0.450801
17	8	5.582661	-0.837973	2.237556
18	42	-5.840403	0.56436	0.136091
19	42	-4.081981	-0.704186	0.037955
20	42	4.18203	0.697803	0.01782
21	42	5.816616	-0.641843	0.121544
22	8	-6.138901	0.352534	-1.944145
23	8	-7.065543	-1.13201	0.453008
24	8	-4.340423	-0.940621	-2.044675
25	6	-5.317411	-0.357056	-2.586148
26	8	4.44638	0.948571	-2.088271
27	8	-5.274208	-2.434345	0.348636
28	6	-6.514017	-2.266084	0.490403
29	7	2.85739	-0.968352	-0.269652
30	8	6.154883	-0.464534	-1.980711
31	8	4.633307	-2.343964	-0.148368
32	6	5.389419	0.305002	-2.619502
33	6	3.365392	-2.20699	-0.271277
34	6	0.597414	-1.826097	-0.486288
35	6	2.488845	-3.335121	-0.396722
36	6	1.158218	-3.158287	-0.495015
37	1	2.943348	-4.319908	-0.400472
38	1	0.464805	-3.986205	-0.583689
39	1	4.520376	-0.261162	3.859033
40	1	5.553075	0.419991	-3.697708
41	1	7.375313	2.984063	0.663991
42	1	-4.57047	0.177187	3.86829
43	1	-7.145638	-3.144401	0.654871
44	1	-5.460141	-0.470869	-3.664968

45	8	-0.617967	-1.577133	-0.562605
46	8	0.527517	1.877732	-0.513017
47	7	-1.534615	0.979147	-0.362006
48	7	1.506528	-0.82428	-0.390782
49	1	-1.146152	0.011193	-0.422294
50	1	1.177569	0.153474	-0.419275

References

1. Wilkinson, L. A.; McNeill, L.; Meijer, A. J. H. M.; Patmore, N. J., *J. Am. Chem. Soc.* **2013**, *135*, 1723.
2. Gaussian 09, Revision C.01, Frisch, M. J.; Trucks, G. W.; Schlegel, H. B.; Scuseria, G. E.; Robb, M. A.; Cheeseman, J. R.; Scalmani, G.; Barone, V.; Mennucci, B.; Petersson, G. A.; Nakatsuji, H.; Caricato, M.; Li, X.; Hratchian, H. P.; Izmaylov, A. F.; Bloino, J.; Zheng, G.; Sonnenberg, J. L.; Hada, M.; Ehara, M.; Toyota, K.; Fukuda, R.; Hasegawa, J.; Ishida, M.; Nakajima, T.; Honda, Y.; Kitao, O.; Nakai, H.; Vreven, T.; Montgomery, Jr., J. A.; Peralta, J. E.; Ogliaro, F.; Bearpark, M.; Heyd, J. J.; Brothers, E.; Kudin, K. N.; Staroverov, V. N.; Kobayashi, R.; Normand, J.; Raghavachari, K.; Rendell, A.; Burant, J. C.; Iyengar, S. S.; Tomasi, J.; Cossi, M.; Rega, N.; Millam, J. M.; Klene, M.; Knox, J. E.; Cross, J. B.; Bakken, V.; Adamo, C.; Jaramillo, J.; Gomperts, R.; Stratmann, R. E.; Yazyev, O.; Austin, A. J.; Cammi, R.; Pomelli, C.; Ochterski, J. W.; Martin, R. L.; Morokuma, K.; Zakrzewski, V. G.; Voth, G. A.; Salvador, P.; Dannenberg, J. J.; Dapprich, S.; Daniels, A. D.; Farkas, Ö.; Foresman, J. B.; Ortiz, J. V.; Cioslowski, J.; Fox, D. J. Gaussian, Inc., Wallingford CT, 2009.
3. Zhao, Y.; Truhlar, D. G., *Theor. Chem. Acc.* **2008**, *120*, 215.
4. (a) McLean, A. D.; Chandler, G. S., *J. Chem. Phys.* **1980**, *72*, 5639; (b) Wachters, J. H., *J. Chem. Phys.* **1970**, *52*, 1033; (c) Hay, P. J., *J. Chem. Phys.* **1977**, *66*, 4377.
5. Andrae, D.; Haeussermann, U.; Dolg, M.; Preuss, H., *Theor. Chim. Acta* **1990**, *77*, 123.